Received: 22 March 2016 | Revised: 29 June 2017 | Accepted: 30 June 2017

DOI: 10.1111/mec.14253

ORIGINAL ARTICLE

WILEY MOLECULAR ECOLOGY

Allopatric speciation despite historical gene flow: Divergence and hybridization in *Carex furva* and *C. lucennoiberica* (Cyperaceae) inferred from plastid and nuclear RAD-seq data

Enrique Maguilla[1] | Marcial Escudero[2] | Andrew L. Hipp[3,4] | Modesto Luceño[1]

[1]Universidad Pablo de Olavide, Seville, Spain

[2]Departamento de Biología Vegetal y Ecología, Universidad de Sevilla, Seville, Spain

[3]The Morton Arboretum, Lisle, IL, USA

[4]Botany Department, Field Museum of Natural History, Chicago, IL, USA

Correspondence
Enrique Maguilla, Universidad Pablo de Olavide, Seville, Spain.
Email: emagsal@gmail.com

Funding information
Spanish Government, Grant/Award Number: AP2012-2189, CGL2012-38744, CGL2016-77401-P; European Community Research Infrastructures Program, Grant/Award Number: GB-TAF-2523; Junta de Andalucía of Spain, Grant/Award Number: RNM2763; National Science Foundation, Grant/Award Number: 1255901

Abstract

Gene flow among incipient species can act as a creative or destructive force in the speciation process, generating variation on which natural selection can act while, potentially, undermining population divergence. The flowering plant genus *Carex* exhibits a rapid and relatively recent radiation with many species limits still unclear. This is the case with the Iberian Peninsula (Spain and Portugal)-endemic *C. lucennoiberica*, which lay unrecognized within *Carex furva* until its recent description as a new species. In this study, we test how these species were impacted by interspecific gene flow during speciation. We sampled the full range of distribution of *C. furva* (15 individuals sampled) and *C. lucennoiberica* (88 individuals), sequenced two cpDNA regions (*atp*I-*atp*H, *psb*A-*trn*H) and performed genomic sequencing of 45,100 SNPs using restriction site-associated DNA sequencing (RAD-seq). We utilized a set of partitioned *D*-statistic tests and demographic analyses to study the degree and direction of introgression. Additionally, we modelled species distributions to reconstruct changes in range distribution during glacial and interglacial periods. Plastid, nuclear and morphological data strongly support divergence between species with subsequent gene flow. Combined with species distribution modelling, these data support a scenario of allopatry leading to species divergence, followed by secondary contact and gene flow due to long-distance dispersal and/or range expansions and contractions in response to Quaternary glacial cycles. We conclude that this is a case of allopatric speciation despite historical secondary contacts, which could have temporally influenced the speciation process, contributing to the knowledge of forces that are driving or counteracting speciation.

KEYWORDS
migration, network analysis, niche modelling, Pleistocene, speciation reversal, vicariance

1 | INTRODUCTION

Gene flow is generally thought of as a force counteracting population divergence (Runemark, Hey, Hansson, & Svensson, 2012). Increased rates of gene flow are expected on average to increase genetic and phenotypic similarities among diverged populations (e.g., Felsenstein, 1976; Hendry, Day, & Taylor, 2001; Hendry & Taylor, 2004), and the strength of intraspecific differentiation correlates in at least some taxa with speciation rates (Harvey et al., 2017). Gene flow may even counteract the effects of local selection, decreasing the fitness of divergent populations by migration of alleles beyond the range in which they are adaptive (Bolnick & Nosil, 2007; García-Ramos & Kirkpatrick, 1997). Stated another way, hybridization is generally thought of as a homogenizing process (Latch, Harveson,

King, Hobson, & Rhodes, 2006; Oliveira, Godinho, Randi, & Alves, 2008). Thus, although hybridization can increase genetic diversity and thus reduce extinction risk in endangered species—for example, in a population suffering a bottleneck (Hedrick & Fredrickson, 2010)—hybridization is more commonly considered a threat to species of conservation concern due to the risk of genetic swamping and consequent extinction of the species.

These facts notwithstanding, gene flow probably very rarely disrupts divergence among lineages (Räsänen & Hendry, 2008), and it can in fact act as a creative force promoting speciation (Abbott et al., 2013; Fitzpatrick, Ryan, Johnson, Corush, & Carter, 2015; Marques, Draper, Riofrío, & Naranjo, 2014; Soltis & Soltis, 2009; Stankowski & Streisfeld, 2015). Hybridization among lineages is common (e.g., Eaton, Hipp, González-Rodríguez, & Cavender-Bares, 2015; Mallet, 2005; McVay, Hipp, & Manos, 2017) and is usually presumed to have neutral ecological and morphological effects (Räsänen & Hendry, 2008; Van Valen, 1976). Even hybrid speciation has been demonstrated to be quite rapid in allopolyploid hybrid speciation (Abbott et al., 2013; Soltis, 2013). Genes or alleles that are adaptive to certain conditions or ecological niches can be transferred from one species to another (Hedrick, 2013; Lewontin & Birch, 1966; Whitney, Randell, & Rieseberg, 2010). This is more common in incipient or recently radiated species, transferring adaptive alleles that can shape rapid divergence (e.g., Lamichhaney et al., 2015; Pardo-Diaz et al., 2012; The Heliconius Genome Consortium 2012).

The genus *Carex* L. (Cyperaceae), with more than 2,000 species (Global Carex Group 2015; Judd, Campbell, Kellogg, Stevens, & Donoghe, 2007), is one of the largest genera of angiosperms and one that has experienced a relatively fast radiation (Escudero & Hipp, 2013; Escudero, Hipp, Waterway, & Valente, 2012). The sheer size of the genus and its perceived morphological homogeneity have made it a taxonomic challenge. Moreover, the genus appears to harbour incipient or very young species whose morphological limits are sometimes unclear (e.g., Gehrke, Martín-Bravo, Muasya, & Luceño, 2010; Jiménez-Mejías, Luceño, & Martín-Bravo, 2014; Whitkus, 1988, 1992), which has led to erroneous attribution of inadequately characterized morphological variation to historical hybridization (Cayouette & Catling, 1992; Escudero, Eaton, Hahn, & Hipp, 2014). One such case appears to be within the species *Carex furva* Webb, in which two previously discovered "morphogroups" or groups of populations with clear synapomorphies (Luceño, 1986) were suggestive of incipient or recent speciation, one comprising populations in the centre-northern Iberian Peninsula, and another comprising populations in the southern Iberian Peninsula. Initially, the presence of morphologically intermediate individuals in the southern Iberian Peninsula made difficult the establishment of clear limits between the morphogroups (Luceño, 1986). Nevertheless, a recent and more exhaustive morphological and molecular study led to the description of part of the variability of *C. furva* as a new species, *C. lucennoiberica* Maguilla & M. Escudero (Maguilla & Escudero, 2016). This speciation event seems to have been influenced by gene flow among diverging species.

This study investigates the speciation process of two very closely related and sister species, *C. furva* and *C. lucennoiberica*. We address how gene flow shaped this speciation process and how it is currently shaping these young species, whether by increasing, decreasing or even maintaining levels of differentiation. Additionally, we aimed to test the role of Sierra Nevada as a refugium during glaciations for these two species.

2 | MATERIALS AND METHODS

2.1 | Study species

Carex furva and *C. lucennoiberica* (Cyperaceae) are reciprocally monophyletic sister species within *Carex* section *Glareosae* G. Don (Maguilla & Escudero, 2016; Maguilla, Escudero, Waterway, Hipp, & Luceño, 2015). Both species are endemic to the Iberian Peninsula (in the case of *C. furva* only from Sierra Nevada, Granada, Spain; Maguilla & Escudero, 2016), where they inhabit high siliceous mountains from 1,800 to 3,100 m above sea level (Luceño, 2008; Maguilla & Escudero, 2016). These species grow in cool environments, only in microclimates where snow persists the longest throughout the year. These specific habitat requirements have led to a narrow distribution, discontinuous in the case of *C. lucennoiberica* (Figure 1), that we would expect to render the species highly sensitive to environmental or climatic changes.

2.2 | DNA sampling and sequencing

A total of 88 individuals of *C. lucennoiberica* and 16 of *C. furva* were sampled (Table 1). Additionally, we included 15 individuals from a morphologically intermediate population in Sierra Nevada (Granada, Spain; population H, Figure 1), which was described as a possible hybrid population in a previous study (Maguilla & Escudero, 2016). Twelve to 16 individuals per population across the range of each species were included (Figure 1, Table 1). The exceptions were two critically endangered populations of *C. lucennoiberica* in Portugal (Covilhã, Serra da Estrela, L4) and Spain (Madrid, Sierra de Guadarrama, L8), comprising only one and seven individuals, respectively (Table 1, Figure 1). Because of the scarce morphological variability in *C. furva* (Maguilla & Escudero, 2016) and its restricted distribution, we included only one population of this species.

DNA was extracted from silica-dried leaves of individuals collected in the field and leaves of specimens from nine herbaria (BABY, BM, DAO, H, M, MHA, RSA, UPOS and WTU; Index Herbariorum (Thiers, 2015)) using the DNeasy Plant Mini Kit (Qiagen, Valencia, CA, USA). Two cpDNA regions were PCR-amplified and sequenced: *atp*IH and *psb*A-*trn*H. These regions were shown to be the most informative in a pilot study with nine commonly used cpDNA markers: 5'*trn*K intron (Escudero & Luceño, 2009), *atp*I-*atp*H (Shaw, Lickey, Schilling, & Small, 2007), *mat*K (Ford et al., 2009), *ndh*J-*trn*F (Shaw et al., 2007), *psb*A-*trn*H (Sang, Crawford, & Stuessy, 1997; Tate & Simpson, 2003), *rpl*32-*trn*L (Shaw et al., 2007), *rps16* (Shaw et al., 2005), *trn*C-*ycf6* (Shaw et al., 2005) and *ycf6*-*psb*M (Shaw et al., 2005). The *atp*IH region was amplified using *atp*I and *atp*H primers (Shaw et al., 2007) following PCR conditions described

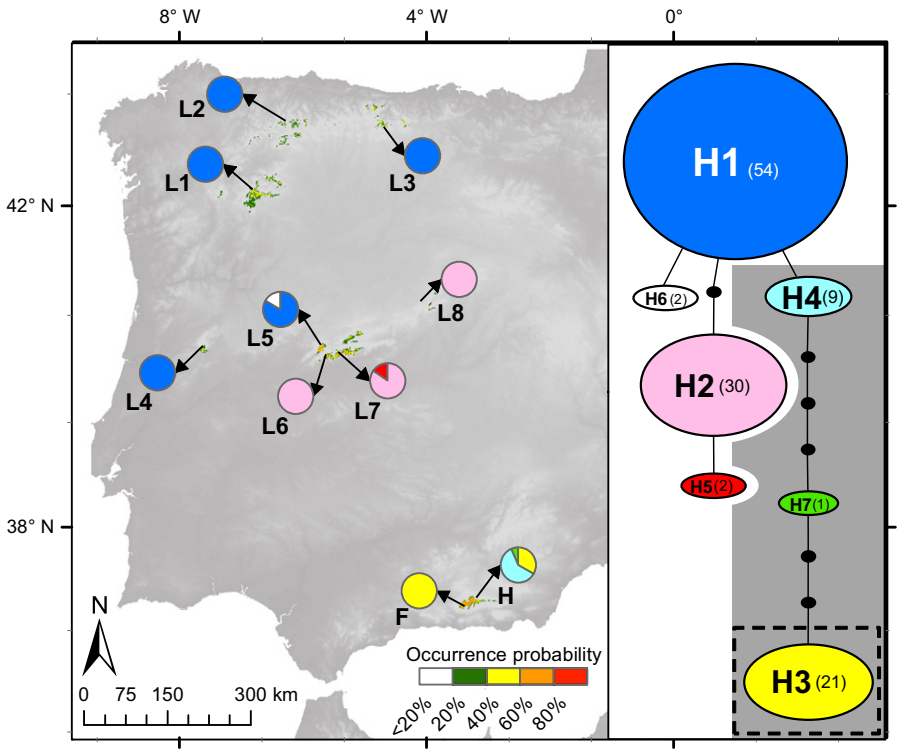

FIGURE 1 Map showing the 13 sampled populations across the full distribution of *Carex furva* and *C. lucennoiberica*. L1 to L8 indicate *C. lucennoiberica* populations, F for *C. furva* and H for the hybrid population. Pie charts indicate haplotypes (blue for H1, pink for H2, yellow for H3, light blue for H4, red for H5, white for H6 and green for H7). Occurrence probability of *C. lucennoiberica* is also shown as indicated in the colour legend, as estimated using MAXENT v.3.3 under current climatic conditions. The haplotype network in the right side of the map was reconstructed in TCS using *atp*IH and *psb*A-*trn*H cpDNA sequences (the same colours than in the map are shown). Numbers in parenthesis indicate how many individuals (of the 119 sampled) display each haplotype. Black dots represent unsampled or extinct haplotypes, and lines refer to single mutational steps. Grey shadow represents hybrid haplotypes and dashed square the only *C. furva* haplotype (H3)

by the authors in Shaw et al. (2007). Reactions with a final volume of 25 μl contained: 2.5 μl 10 × PCR buffer, 1.6 μl $MgCl_2$ at 50 mM, 2 μl dNTPs at 10 mM, 1 μl of each primer at 10 μM, 1 μl of 1 × BSA, 0.3 μl of Taq DNA polymerase at 5 U/μl and 1 μl of DNA. For the *psb*A-*trn*H region, primers *psb*AF (Sang et al., 1997) and *trn*H2 (Tate & Simpson, 2003) were used, and PCR was conducted using the same reagent concentrations as for the *atp*IH region, with thermal cycling conditions as follows: 5 min of initial DNA denaturation at 80°C followed by 35 cycles with 30 s of denaturation at 94°C, 30 s of primer annealing at 53°C, and extension at 72°C for 1 min, finishing with 10 min of final extension at 72°C. All reactions were conducted in a Bio-Rad T100TM Thermal Cycler, and products were purified using ExoSAP-IT (USB, Cleveland, OH, USA). Sequencing followed Escudero and Luceño (2009).

2.3 | Phylogenetic analyses of cpDNA sequences and haplotype network

All 119 samples (*C. furva*, *C. lucennoiberica* and morphologically intermediate population [hereafter intermediate population], H; Table 1) were included in phylogenetic analyses, as well as one sample each of *C. brunnescens* (SWE), *C. canescens* (SPA 1) and *C. lachenalii* (SPA 1; Table 1) as the outgroup, based on previous phylogenetic study of *Carex* section *Glareosae* (Maguilla et al., 2015). Sequences for *atp*IH and *psb*A-*trn*H were assembled and edited separately using GENEIOUS v.6.1.7 (Biomatters, Auckland, New Zealand), then aligned with MUSCLE (Edgar, 2004) before being concatenated in GENEIOUS v.6.1.7. Indels were coded manually as presence or absence at the end of the data matrix following the "simple indel coding" (Simmons & Ochoterena, 2000).

Bayesian inference (BI) was performed using MRBAYES 3.2 (Ronquist et al., 2012) within GENEIOUS v.6.1.7. Two analyses of four Metropolis-coupled Markov chains (MCMC) were run for 5 million generations. Substitution models were selected for each of the two cpDNA regions separately, based on the highest Akaike Information Criterion weights (AICw; Akaike, 1974) calculated in JMODELTEST 2.1.3 (Darriba, Taboada, Doallo, & Posada, 2012). Indels were analysed as a different data partition using a F81-like model following Jiménez-Mejías, Martín-Bravo, and Luceño (2012). Posterior probabilities (PP) were calculated as clade support. Unweighted maximum parsimony (MP) analyses were conducted on the concatenated matrix using TNT 1.1 software (Goloboff, Farris, & Nixon, 2008), and maximum-likelihood (ML) analysis in RAXML 7.2.6 (Stamatakis, Hoover, & Rougemont, 2008) using bootstrap calculation (BS) as clades support, using the

TABLE 1 Studied material. The "botanical country" where the species was collected following Brummitt (2001) and population names for *Carex furva* and *Carex lucennoiberica* (in parenthesis) are indicated. Locality, date and altitude of collection, voucher (including herbarium acronym and code of the specimen as in Index Herbariorum (Thiers, 2015) when available), NCBI GenBank accession number for each amplified cpDNA region (*atp*IH and *psb*A-*trn*H), and accession number of the RAD-seq data are also shown

Population	Number of samples	Locality (long, lat). Collection date. Altitude.	Voucher (herbarium code)	Haplotypes	NCBI accession number		RAD-seq accession number
					*atp*I-*atp*H	*psb*A-*trn*H	
C. brunnescens (Pers.) Poir.							
SWE	1	Sweden: Jämtland, Enafors, along path. 13/VIII/1960. 550 m.s.m.	H. Smith, 3887 (BM)		KU997978	KU998112	
C. canescens L.							
SPA 1	1	Spain: Lérida, central Pyrenees, Arán valley, Tredós, Noguera de Ruda, silted up lagoon below Lago Mayor de Saboredo. (0.967956, 42.617800). VIII/2011.	M. Luceño, 17ML11 (UPOS-5304)		KU997977	KU998111	
SPA 2	1	Spain: Lérida, central Pyrenees, Tredós, Aguamoix river valley, path from Tredós' Spa to Colomers' lakes, besides first lake. (0.924778, 42.629444). 16/VIII/2012. 2040 m.s.m.	E. Maguilla et al., 34EMS12 (UPOS-5045)				SAMN04884654
C. furva Webb							
SPA (F)	15	Spain: Granada, Sierra Nevada, near Veleta mountain, along the stream to Laguna de Los Vasares. (−3.368902, 37.049531). 08/VIII/2013. 3098–3126 m.s.m.	E. Maguilla and J. M. G. Cobos, 31EMS13 (UPOS-5132)	15 ind. H3	KU997985, KU997992, KU997999, KU998006, KU998013, KU998020, KU998027, KU998037, KU998045, KU998066, KU998074, KU998076, KU998082, KU998090, KU998097	KU998119, KU998126, KU998133, KU998140, KU998147, KU998154, KU998161, KU998171, KU998179, KU998200, KU998208, KU998210, KU998216, KU998224, KU998231	SAMN04884660
SPA (F)	1	Spain: Granada, Sierra Nevada, Lakes and streams near to reservoir of Yeguas. (−3.379389, 37.055042). 19/VIII/2006. 2860 m.s.m.	P. Jiménez-Mejías and M. Escudero, 161PJM06 (UPOS-3833)	1 ind. H3	KU998038	KU998172	
C. furva × *lucennoiberica* (Hybrid population)							
SPA (H)	15	Spain: Granada, Sierra Nevada, from Peñón negro to Siete Lagunas. (−3.294219, 37.036703). 09/VIII/2013. 2952 m.s.m.	E. Maguilla and J. M. G. Cobos, 34EMS13 (UPOS-5135)	5 ind. H3 9 ind. H4 1 ind. H7	KU997986, KU997993, KU998000, KU998007, KU998014, KU998021, KU998028, KU998029, KU998052, KU998059, KU998067, KU998075, KU998083, KU998091, KU998098	KU998120, KU998127, KU998134, KU998141, KU998148, KU998155, KU998162, KU998163, KU998186, KU998193, KU998201, KU998209, KU998217, KU998225, KU998232	SAMN04884661, SAMN04884662, SAMN04884663

(Continues)

TABLE 1 (Continued)

Population	Number of samples	Locality (long, lat). Collection date. Altitude.	Voucher (herbarium code)	Haplotypes	NCBI accession number		RAD-seq accession number
					*atp*I-*atp*H	*psb*A-*trn*H	
C. lachenalii Schkuhr							
SPA 1	1	Spain: Lérida, Tredós, Arán Valley, Cirque of Colomers. (0.920722, 42.599889). VIII/2011.	M. Luceño, 13ML11 (UPOS-5051)		KU997979	KU998113	
SPA 2	1	Spain: Lérida, Tredós, superior lake of Colomers, lake Port de Colomers. (0.920722, 42.599889). 17/VIII/2012. 2409 m.s.m.	E. Maguilla et al. 37EMS12 (UPOS-5046)				SAMN04884655
C. lucennoiberica Maguilla & M. Escudero							
POR (L4)	1	Portugal: Guarda, Serra da Estrela, Alto das Salgadeiras, near Pico Torre, below the reservoir. (−7.607519, 40.327047). 02/VIII/2012.	E. Maguilla et al., 28EMS12 (UPOS)	1 ind. H1	KU998084	KU998218	SAMN04884659
SPA (L1)	15	Spain: Orense, Sierra Segundera, between Peña Trevinca and Jancional mountains. (−6.803569, 42.237971). 2085 m.s.m. 24/VIII/2013.	E. Maguilla, 39EMS13 (UPOS-5117)	15 ind. H1	KU997982, KU997995, KU998002, KU998009, KU998016, KU998023, KU998033, KU998041, KU998049, KU998055, KU998063, KU998071, KU998079, KU998087, KU998094	KU998116, KU998129, KU998136, KU998143, KU998150, KU998157, KU998167, KU998175, KU998183, KU998189, KU998197, KU998205, KU998213, KU998221, KU998228	SAMN04884666
SPA (L2)	15	Spain: Oviedo, Sierra de Somiedo, Natural Park of Somiedo, base of Cornón mountain. (−6.303181, 43.031189). 23/VIII/2013. 2012 m.s.m.	E. Maguilla and T. Villaverde, 36EMS13 (UPOS-5136)	15 ind. H1	KU997980, KU997987, KU997994, KU998001, KU998008, KU998031, KU998039, KU998047, KU998053, KU998060, KU998061, KU998069, KU998077, KU998085, KU998092	KU998114, KU998121, KU998128, KU998135, KU998142, KU998165, KU998173, KU998181, KU998187, KU998194, KU998195, KU998203, KU998211, KU998219, KU998226	SAMN04884665
SPA (L3)	13	Spain: Palencia, Curavacas mountain. (−4.683888, 42.983333). 30/VIII/2007. 2000 m.s.m.	S. Martín-Bravo and P. Jiménez-Mejías, 172SMB07 (UPOS-5054)	13 ind. H1	KU997981, KU997988, KU998015, KU998022, KU998032, KU998040, KU998048, KU998054, KU998062, KU998070, KU998078, KU998086, KU998093	KU998115, KU998122, KU998149, KU998156, KU998166, KU998174, KU998182, KU998188, KU998196, KU998204, KU998212, KU998220, KU998227	SAMN04884668

(Continues)

TABLE 1 (Continued)

Population	Number of samples	Locality (long, lat). Collection date. Altitude.	Voucher (herbarium code)	Haplotypes	NCBI accession number		RAD-seq accession number
					*atp*I-*atp*H	*psb*A-*trn*H	
SPA (L5)	11	Spain: Ávila, Sierra de Béjar, between La Covatilla ski resort and Collado Bonal. (−5.695783, 40.339886). 20/VII/2011. 2250 m.s.m.	M. Luceño, 11ML11 (UPOS-5052)	9 ind. H1 2 ind. H6	KU997989, KU997996, KU998003, KU998010, KU998017, KU998024, KU998034, KU998042, KU998050, KU998056, KU998064	KU998123, KU998130, KU998137, KU998144, KU998151, KU998158, KU998168, KU998176, KU998184, KU998190, KU998198	SAMN04884667
SPA (L5)	1	Spain: Ávila, Sierra de Béjar, Hoyo Malillo cirque. (−5.734550, 40.295008). 07/VIII/2010. 2300 m.s.m.	M. Luceño et al., 21ML10 (UPOS-4319)	1 ind. H1	KU998046	KU998180	
SPA (L6)	12	Spain: Ávila, Sierra del Barco, Alto de Castilfrío. (−5.616602, 40.225602). 15/VII/2012. 2210 m.s.m.	E. Maguilla et al., 23EMS12 (UPOS-5039)	12 ind. H2	KU997983, KU997990, KU997997, KU998004, KU998011, KU998018, KU998025, KU998035, KU998072, KU998080, KU998088, KU998095	KU998117, KU998124, KU998131, KU998138, KU998145, KU998152, KU998159, KU998169, KU998206, KU998214, KU998222, KU998229	SAMN04884658
SPA (L7)	13	Spain: Ávila, Sierra de Gredos, El Venteadero. (−5.299869, 40.253713). 14/VII/2012. 2476 m.s.m.	E. Maguilla and M.Luceño, 15EMS12 (UPOS-5037)	11 ind. H2 2 ind. H5	KU997984, KU997991, KU997998, KU998005, KU998043, KU998051, KU998057, KU998065, KU998068, KU998073, KU998081, KU998089, KU998096	KU998118, KU998125, KU998132, KU998139, KU998177, KU998185, KU998191, KU998199, KU998202, KU998207, KU998215, KU998223, KU998230	SAMN04884656, SAMN04884657
SPA (L8)	7	Spain: Madrid, Sierra de Guadarrama, Risco de los Pájaros. (−3.951164, 40.858708). 22/VIII/2013. 2323 m.s.m.	E. Maguilla and T. Villaverde, 35EMS13 (UPOS-5141)	7 ind. H2	KU998012, KU998019, KU998026, KU998030, KU998036, KU998044, KU998058	KU998146, KU998153, KU998160, KU998164, KU998170, KU998178, KU998192	SAMN04884664

GTRGAMMA model, with 10,000 fast bootstraps followed by slow ML optimization (default "–f a" search). Details of phylogenetic reconstruction follow Maguilla et al. (2015).

The cpDNA haplotype network was reconstructed for the 119 ingroup samples (*C. furva*, *C. lucennoiberica* and intermediate population; Table 1) using the concatenated matrix of *atp*IH and *psb*A-*trn*H sequences, following the statistical parsimony method (Templeton, Crandall, & Sing, 1992) as implemented in TCS 1.21 (Clement, Posada, & Crandall, 2000). Indels were coded following "simple indel coding" in Simmons and Ochoterena (2000), and gaps were treated as missing data in the TCS analysis.

2.4 | Restriction site-associated DNA sequencing (RAD-seq) analyses

From all ingroup samples included in phylogenetic studies (Table 1), we selected a subsample of 13 individuals including one sample per population except for two populations in Spain: Ávila, Sierra de Gredos (L7, Table 1; included two samples) and Granada, Sierra Nevada (population H, the one with intermediate morphology; three samples included), which were oversampled to represent each of the detected haplotypes (see Results). In the population in Spain, Ávila, Sierra de Béjar (L5), we could include only one of the two detected haplotypes due to lack of well-preserved material suitable for RAD-seq (Table 1). We included one sample of *C. canescens* (SPA 2) and one of *C. lachenalii* (SPA 2) as outgroup (Table 1).

DNA was extracted from silica-dried specimens as specified above. Preparation of RAD-seq libraries using restriction enzyme *Pst*I from genomic DNA followed by sonication and barcoding was performed by Floragenex Inc. (Eugene, OR, USA) following Baird et al. (2008) using barcodes specific to each sample. We used PYRAD v.2.13 (Eaton, 2014) for demultiplexing and clustering, following methods in Hipp et al. (2014), using a clustering threshold of 90% similarity and minimum sequencing depth of 10 sequences per locus for within-sample clustering; 90% similarity and a minimum of four individuals per locus for among-individual clustering. We investigated the effects of clustering threshold and minimum number of individuals per locus (as recommended in Ree & Hipp, 2015) but found essentially no effect on topology, and very little effect on support values and branch lengths; consequently, we do not report on these alternative analyses in this study.

Loci were concatenated to make a supermatrix using the package RADAMI v.1.0-3 (Hipp, 2014) in R v.3.2.2 (R Core Team 2015), which was analysed using Bayesian inference (BI) in EXABAYES v.1.5 (Aberer, Kobert, & Stamatakis, 2014) under an unpartitioned GTRGAMMA model and posterior probability supports for clades. Two independent runs of 10 million generations and four chains were run and with 25% of burn-in. We used the postprocessing tools to obtain a consensus tree (consense function), establish clade support (credibleSet function) and to check parameters sampling (postProcparam function). Our data set was also analysed using maximum likelihood in RAXML 7.2.6 (Stamatakis et al., 2008) under an unpartitioned GTRCAT model and bootstrap supports for clades calculated using 200 nonparametric bootstrap replicates. Additionally, a network analysis was performed using SNPs from RAD-seq data in NETVIEW v.1.1 (Neuditschko, Khatkar, & Raadsma, 2012; Steinig, Neuditschko, Khatkar, Raadsma, & Zenger, 2016) as implemented in R v.3.2.2 (R Core Team 2015). A $k = 10$ value was applied after testing for the best k using mutual k-nearest neighbour graphs (mkNNGs).

Finally, to test for the genetic structure of the species, discriminant analysis of principal components (DAPC; Jombart et al., 2010) was performed using SNPs as the input on R package ADEGENET v.2.0.1 (Jombart, 2008). The optimal number of genetic clusters was estimated using *find.cluster* function in ADEGENET.

2.5 | Patterson's *D*-statistic test for introgression

To detect historical introgression between main lineages of the resulting phylogeny from RAD-seq analyses, we used the four taxon *D*-statistic (Durand, Patterson, Reich, & Slatkin, 2011; Green et al., 2010) as implemented in PYRAD v.2.13 (Eaton, 2014). The *D*-statistic test is based on the expectation that introgression from a population P3 into either of two populations P1 or P2 can be distinguished from the effects of lineage sorting if the species tree topology is known to be asymmetrical, with this form: (((P1,P2),P3),O), where O is the outgroup. Based on the topology obtained from the phylogenetic analysis using RAD-seq data, the P3 clade, which must fall sister to the P1 and P2 clades, comprised *C. furva* plus a putative hybrid with haplotype H3. We performed the *D*-statistic analysis with every possible combination of the populations/individuals of *C. lucennoiberica* from Portugal (Covilhã, Serra da Estrela, population L4; Table 1) and from Spain such as Ávila, Sierra del Barco (L6), Ávila, Sierra de Béjar (L5) or specimens of the intermediate population from Granada, Sierra Nevada (H) with haplotypes H4 or H7 (as P1); Oviedo, Sierra de Somiedo (L2), Madrid, Sierra de Guadarrama (L8), Palencia, Curavacas Mountain (L3), Orense, Sierra Segundera (L1) or Ávila, Sierra de Gredos (L7) (as P2); specimens of *C. lucennoiberica* and the intermediate population with haplotype H3 from Granada, Sierra Nevada (F and H populations) (as P3, sister to P1 and P2); and the clade formed by *C. canescens* and *C. lachenalii* (as O). We included heterozygous sites in the analyses and ran 1,000 bootstrap iterations for each replicate to get the standard deviation of the *D*-statistic.

We performed a partitioned *D*-statistic test (Eaton & Ree, 2013; Eaton et al., 2015) to infer the direction of introgression. This test is based on the asymmetry of occurrence of derived alleles present in two P3 sublineages or only one of these, and present in lineage P2 or P1 but not both, given the topology (((P1,P2),($P3_1$,$P3_2$)),O). We selected the same samples to represent lineages P1, P2 and O as we had used in the four-taxa *D*-tests, with two exceptions: for P3, we selected $P3_1$ to be the *C. furva*, population F Table 1); and $P3_2$ comprised population H (intermediate) from Granada, Sierra Nevada (Table 1). With this sampling, if the dominant direction of introgression was from one of the Sierra Nevada populations (*C. furva* [$P3_1$] or the intermediate population [$P3_2$]) to the *C. lucennoiberica* populations P1 or P2 (the latter also including intermediate individuals), we

would expect to find introgressed alleles in both P3 populations due to shared ancestry. This is because the split of P1 or P2 from P3 under this scenario would have preceded divergence between the P3 populations, so $P3_1$ and $P3_2$ should share these alleles from an exclusive common ancestor and then introgressed into P1 or P2. Conversely, if the direction of introgression were from P1 or P2 to one of the P3 populations, the other population of P3 would not exhibit these because the introgression occurred after the split of both P3 populations from only one of those populations ($P3_1$ or $P3_2$) to P1 or P2 (Eaton & Ree, 2013; Eaton et al., 2015). Thus, the 5-taxon *D*-statistic tests complements the 4-taxon test in our study by allowing us to evaluate first whether gene flow is present between both species, then whether gene flow from *C. lucennoiberica* may be swamping the species with more restricted distribution, *C. furva*. All *D*-statistic tests were corrected for multiple comparisons using a Holm–Bonferroni correction, using a significance level of $\alpha = 0.01$ as cut-off as recommended in Eaton and Ree (2013).

2.6 | Generalized phylogenetic coalescent demographic analysis

We investigated the demographic history of the species using the generalized phylogenetic coalescent sampler (G-PhoCS; Gronau, Hubisz, Gulko, Danko, & Siepel, 2011) applied to 36,329 RAD-seq loci. Two different sampling strategies were used: one excluding intermediate individuals using a simple topology in which *C. furva* is sister to *C. lucennoiberica* individuals altogether; and an alternative including all samples, where the total-evidence ML tree topology from RAD-seq data, was utilized (Figure 2). The latter case is more complicated topologically: *C. lucennoiberica*, Clade C, is sister to a major clade comprising additional *C. lucennoiberica*, *C. furva* and intermediate individuals, which is subdivided into a subclade containing *C. lucennoiberica* plus two intermediate individuals (clade B) and another subclade containing a single *C. furva* and one intermediate individual (clade A). Default settings described in Gronau et al. (2011) were used for prior distributions of model parameters, with *find-finetunes* = TRUE. We allowed migration between *C. lucennoiberica* and *C. furva* in either direction in the first approach, and between clades A–B and A–C in the second approach, to test for the effect of secondary contacts between *C. furva* and *C. lucennoiberica*, using default migration rate priors.

We ran 180,000 Markov Chain Monte Carlo (MCMC) iterations for four independent runs, sampling parameters every 100 iterations. We assessed convergence using TRACER v.1.6 (Rambaut & Drummond, 2014) and removed the first 10% of recorded values as burn-in.

2.7 | Past and present distribution modelling

To evaluate changes in distribution ranges of *C. furva* and *C. lucennoiberica* due to Quaternary climatic fluctuations, we performed species distribution modelling for both species independently, using maximum entropy analysis in MAXENT v.3.3.3k (Phillips, Anderson, & Schapire, 2006). We downloaded 19 current bioclimatic variables from the WORLDCLIM website (www.worldclim.org; Fick & Hijmans, 2017). Then, we selected uncorrelated variables using a cluster dendrogram analysis in R v.3.2.2 (R Core Team 2015), applying a threshold of 0.6 dissimilarity for the selection of the variables. For the occurrence data of both species, we included herbarium materials and field trips data published by Maguilla and Escudero (2016), totalling seven *C. furva* and 48 *C. lucennoiberica* localities excluding duplicates.

For the estimation of current potential distribution of species, we ran 1,000 bootstrap replicates using 80% of species localities as training data, and the remaining 20% to test the model. Then, we projected resulting distribution models to past climatic conditions assuming stable ecological niche requirements through time, at least

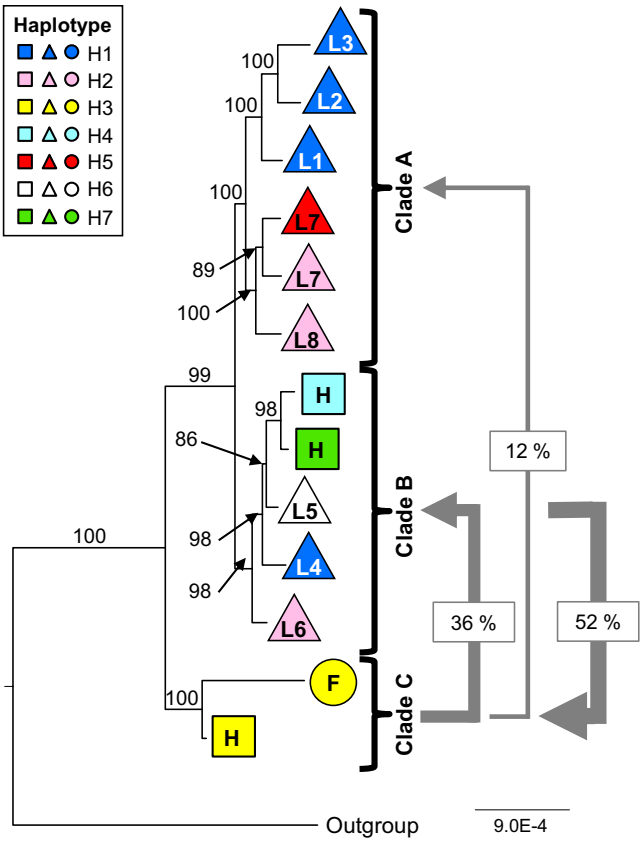

FIGURE 2 Maximum-likelihood (ML) phylogram obtained from RAXML analysis of the RAD-seq sequences. Analysed matrix was obtained using clustering at 90% of similarity, a minimum of 10 sequences per locus as depth coverage per individual and a minimum of at least four individuals having a given locus to maintain it in the final matrix. Values above branches indicate ML bootstrap support. Tip labels indicate population names as in Table 1 using triangles to represent *C. lucennoiberica* individuals, circle for *C. furva* and squares for hybrid individuals. Haplotypes are shown using colours as legend (blue for H1, pink for H2, yellow for H3, light blue for H4, red for H5, white for H6 and green for H7). Scale bar corresponds to substitutions per site. Grey arrows indicate the direction of introgression detected using the *D*-statistic test at .01 significance level showing the percentage of each of the 50 analyses performed that support each scenario of introgression

in the last climatic cycle (Nogués-Bravo, 2009). Projections to the last glacial maximum (LGM, ca. 21 kyr before present) were performed using palaeoclimate data obtained from the Community Climate System Model (CCSM4; Gent et al., 2011) and the Max-Planck-Institut Earth System Model (MPI-ESM-P; Giorgetta et al., 2013) of atmospheric circulation. In the case of the last interglacial period (LIG, ca. 120,000–140,000 years bp), we used palaeoclimatic data published in Otto-Bliesner, Marshall, Overpeck, Miller, and Hu (2006).

3 | RESULTS

3.1 | Phylogenetic analyses of cpDNA sequences

We sequenced *atp*IH and *psb*A-*trn*H regions for all 136 sampled individuals (see matrices in Data S1 and S2). Based on results from JMODELTEST (Darriba et al., 2012) including all *C. furva* and *C. lucennoiberica* samples, plus *C. brunnescens* (SWE), *C. canescens* (SPA 1) and *C. lachenalii* (SPA 1) as outgroup (Table 1), the evolutionary model that best fits for *atp*IH was GTR (AICw = 0.3182 [AICw for GTR+I = 0.2913, for GTR+G = 0.2784, for GTR+I+G = 0.1073]), whereas for *psb*A-*trn*H the selected model was HKY (AICw = 0.2350 [AICw for F81 = 0.1917, for GTR = 0.1094, for HKY+I = 0.0864]). Analyses using the second-best evolutionary model for each partition retrieved the same tree topology and almost the same posterior probability values for all clades (results not shown).

Carex furva and *C. lucennoiberica* constitute an exclusive lineage significantly supported in BI and ML analysis of the combined matrix (1.0 PP/99% ML-BS; Fig. S1). The populations of *C. lucennoiberica* together form an exclusive lineage with significant support (0.98 PP and 99% BS; Fig. S1). The populations of *C. furva* are paraphyletic with respect to samples of the intermediate morphotype with haplotype H3, with significant support (1 PP and 99% BS-ML, 86 BS-MP; Fig. S1). The intermediate morphotype (H) is paraphyletic with respect to all other populations of *C. furva* and *C. lucennoiberica*.

3.2 | Analysis of DNA haplotypes

The cpDNA haplotype network shows seven sampled (four haplotypes in *C. lucennoiberica* [H1, H2, H5 and H6], one in *C. furva* [H3], and three in the hybrid population [H3, H4 and H7]) and six missing haplotypes (Figure 1, but see Table S1 for a full list of haplotypes per individuals). Three major haplotypes are geographically segregated: one from the northern and central-western populations (H1), one from the central-eastern populations (H2) and one (H3) exclusive to the south. Eight mutational steps differentiate H1 (*C. lucennoiberica*) from H3 (*C. furva* and hybrids), while only two steps separate the *C. lucennoiberica* haplotype H1 from H2 (Figure 1). Haplotypes between H1 (*C. lucennoiberica*) and H3 (*C. furva* and intermediate morphotype) were found in the intermediate population in the south (haplotypes H4 and H7), and two minor haplotypes in the central populations of *C. lucennoiberica* (H5 and H6) differing only by one mutational step from H2 and H1, respectively (Figure 1).

3.3 | Restriction site-associated DNA sequencing (RAD-seq) analyses

Individuals in this study are represented by an average of 764,000 sequencing reads (566,000–2,680,000) after quality filtering in PYRAD v.2.13 (Eaton, 2014). After clustering, we recovered 20,200 loci per individual that passed paralog filtering (15,600–32,100). The concatenated matrix of aligned loci including gaps had a total 3,120,000 sites and 45,100 variable sites including indels (of which 11,300 were potentially parsimony informative), with 55.28% missing data. Obtained RAD-seq data are deposited in NCBI SRA.

The BI (Fig. S2) and ML (Figure 2) phylogenies of the RAD-seq matrix show almost the same topology including three major clades: clade A (1.0 PP/100% BS support) containing all northern populations of *C. lucennoiberica* (L1 to L3) and the easternmost central populations (L7 and L8) in a different subclade, both subclades with 1.0 PP/100% BS support. Topology within subclade containing L7–L8 populations differs between BI and ML analyses [((L7-H5,L8-H2)L7-H2) and ((L7-H5, L7-H2)L8-H2), respectively]; clade B (1.0 PP/98% BS), including the westernmost-central populations of *C. lucennoiberica* (L4–L6) and two individuals from the intermediate (H) population from the south with haplotypes H4 and H7 (Figures 1 and 2); and clade C (1.0 PP/100% BS) containing all *C. furva* individuals and individuals in the intermediate population with haplotype H3 (Figures 1 and 2).

Network analysis suggests strong interconnections among *C. lucennoiberica* populations (Figure 3). The only *C. furva* individual is the most isolated, connected only by intermediate individuals (H) with haplotypes H3 and H7, plus population L1 and L6 of *C. lucennoiberica* (haplotype H2). Intermediate individuals present from six to nine connections, where the individual with haplotype H3 is the most isolated among intermediate individuals (Figure 3).

The DAPC analysis using $k = 10$ classified *C. furva* plus the intermediate individual with haplotype H3 as a single genetic group, whereas all *C. lucennoiberica* individuals plus intermediate individuals with haplotype H4 and H7 comprised a second group (Fig. S3).

3.4 | *D*-statistic test for introgression

Four-taxa *D*-statistic tests detected introgression mostly between clades B and C, supported by 88.33% of the 60 tests performed (Table S2). This is congruent with the best-supported pattern of introgression showed by partitioned *D*-statistic test (five-taxa), from central to southern populations, from clade B to clade C (Figure 2; Table S2), which is supported at .01 significance level in 52% of the 50 tests we performed. Two other patterns of introgression were detected from clade C, which consists of southern populations of *C. furva* (F) and the hybrid (H) with haplotype H3, to clade A (12% of tests) and clade B (36% of tests; Figure 2; Table S2).

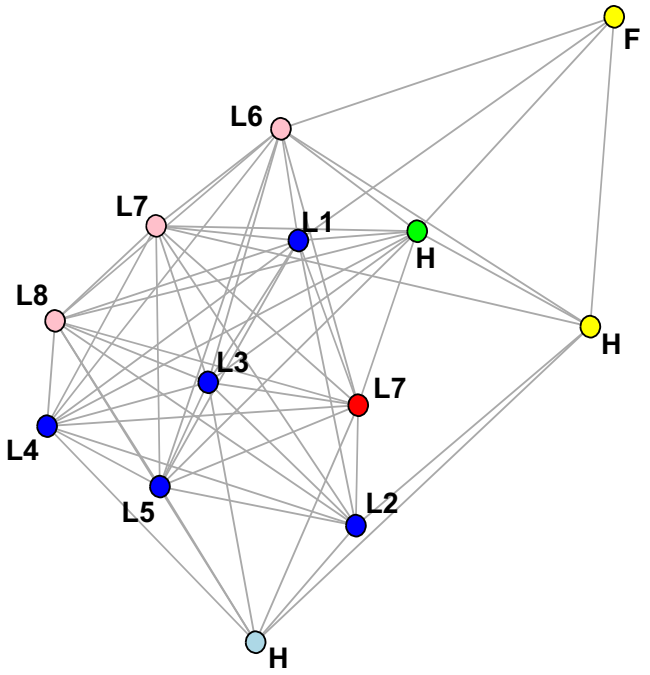

FIGURE 3 Population network of *Carex furva* and *C. lucennoiberica* obtained using NETVIEW v.1.1 in R v.3.2.2. A 21,214 SNPs matrix from RAD-seq was used as input, and a maximum nearest neighbour (NN) of $k = 10$ was used. Node labels indicate population names as in Table 1 (F for *C. furva* individual; H for hybrid individuals; L1–L8 for *C. lucennoiberica*). Haplotypes are shown using colours as in Figure 1 (blue for H1, pink for H2, yellow for H3, light blue for H4, red for H5, white for H6 and green for H7)

3.5 | Demographic analysis

Results from G-PhoCS analysis excluding intermediate individuals show a greater population size for *C. lucennoiberica* (θ = 5.936E-4 [5.8E-4 – 6.1E-4 95% CI]) than for *C. furva* (θ = 8.946E-5 [8.946E-5 – 8E-5 95% CI]) (Fig. S4), with most migration events from *C. lucennoiberica* to *C. furva* [99.9% migrations (98.1%–100%) vs. 0.1% (0–0.4%) in the other direction; Fig. S4]. When analysing migration among the three major clades detected in the BI and ML analyses of the RAD-seq data (Figure 2), most events occurred from clade B (containing *C. lucennoiberica* plus intermediate individuals with haplotypes H4 and H7) to clade C (containing *C. furva* plus a intermediate individual with haplotype H3), representing 98.4% (97.9%–98.8%) of all migration events (Figure 4). Although additional migration patterns are significantly small, we find some migration from clade C to B (0.9%–1.2%), but also from clade A to C (0–0.4%) and C to A (0.3%–0.5%; Figure 4).

3.6 | Distribution modelling analysis

The current distribution for *C. lucennoiberica* as inferred using distribution model, closely reflected the observed distribution of the species, but also included some areas in the Pyrenees (Spain) and in the Atlas Cordillera (Morocco) where this species has never been found (Figure 5). In the case of *C. furva*, the modelled area was much greater than the area of the observed distribution, including most regions predicted for *C. lucennoiberica* except some northwestern points of the Iberian Peninsula, plus the easternmost part of the Sistema Central mountain range in Spain (Figure 5). Both models were highly supported by an average area under the receiver-operating characteristic curve (AUC) of 0.997 (0.001 *SD*) and 1.0 (~0 *SD*) for *C. lucennoiberica* and *C. furva*, respectively. The most informative variables were bio8 (mean temperature of the wettest quarter) and bio1 (annual mean temperature).

Past projections for *C. lucennoiberica* showed a greater range during the LGM in the northern Iberian Peninsula than is projected for the current range, whereas during the last interglacial period (LIG), the average probability of occurrence increases considerably in southern latitudes (Sierra Nevada and Morocco), with on average smaller distribution range of the species than in the LGM, but still larger than the present potential distribution (Figures 5 and 6). In the case of *C. furva*, the general occupancy seems to be almost invariable during glacial and interglacial periods, although probability of occurrence increases in higher altitudes during the last glacial maximum (Figure 6). The CCSM4 and MPI-ESM-P models for the LGM retrieved almost the same pattern, although probabilities of niche suitability changed moderately (data not shown).

4 | DISCUSSION

4.1 | Origin and differentiation of *Carex furva* and *Carex lucennoiberica*

Alpine plants of the Mediterranean Basin have mostly followed a common biogeographic pathway in response to climate changes during the Quaternary: migration to lowlands during glaciations and to higher altitudes during warmer periods (Hewitt, 2000; Van Andel & Tzedakis, 1996; Vargas, 2003). The evolutionary history of *C. furva* and *C. lucennoiberica* is, in part, one more such example. The origin of the *C. furva*–*C. lucennoiberica* clade in the Pleistocene to early Pliocene (ca. 1.98 Ma; Maguilla et al. in review) suggests a broader distribution of both species during glacial periods (Figure 6), followed by relative isolation in high mountain refugia during interglacial periods such as the present (Figure 1). This pattern of range contraction at higher elevations is well documented in other alpine plant species (Pauli, Gottfried, & Grabherr, 1996; Walther, 2003; Walther, Beißner, & Burga, 2005).

The Iberian, Italic and Balkan Peninsulas as well as the Caucasus region all acted as floristic refugia in Europe during glacial periods (Hewitt, 2004; Petit et al., 2003; Taberlet, Fumagalli, Wust-Saucy, & Cosson, 1998), while the highest alpine altitudes serve as refugia for alpine species during interglacial periods (Bennett, Tzedakis, & Willis, 1991; Brochmann, Gabrielsen, & Nordal, 2003; Tribsch & Schönswetter, 2003). The resulting disjunct distribution we find in *C. lucennoiberica* (Figure 1) is found in other medium altitude montane *Carex* species such as *C. reuteriana* (Jiménez-Mejías, Escudero,

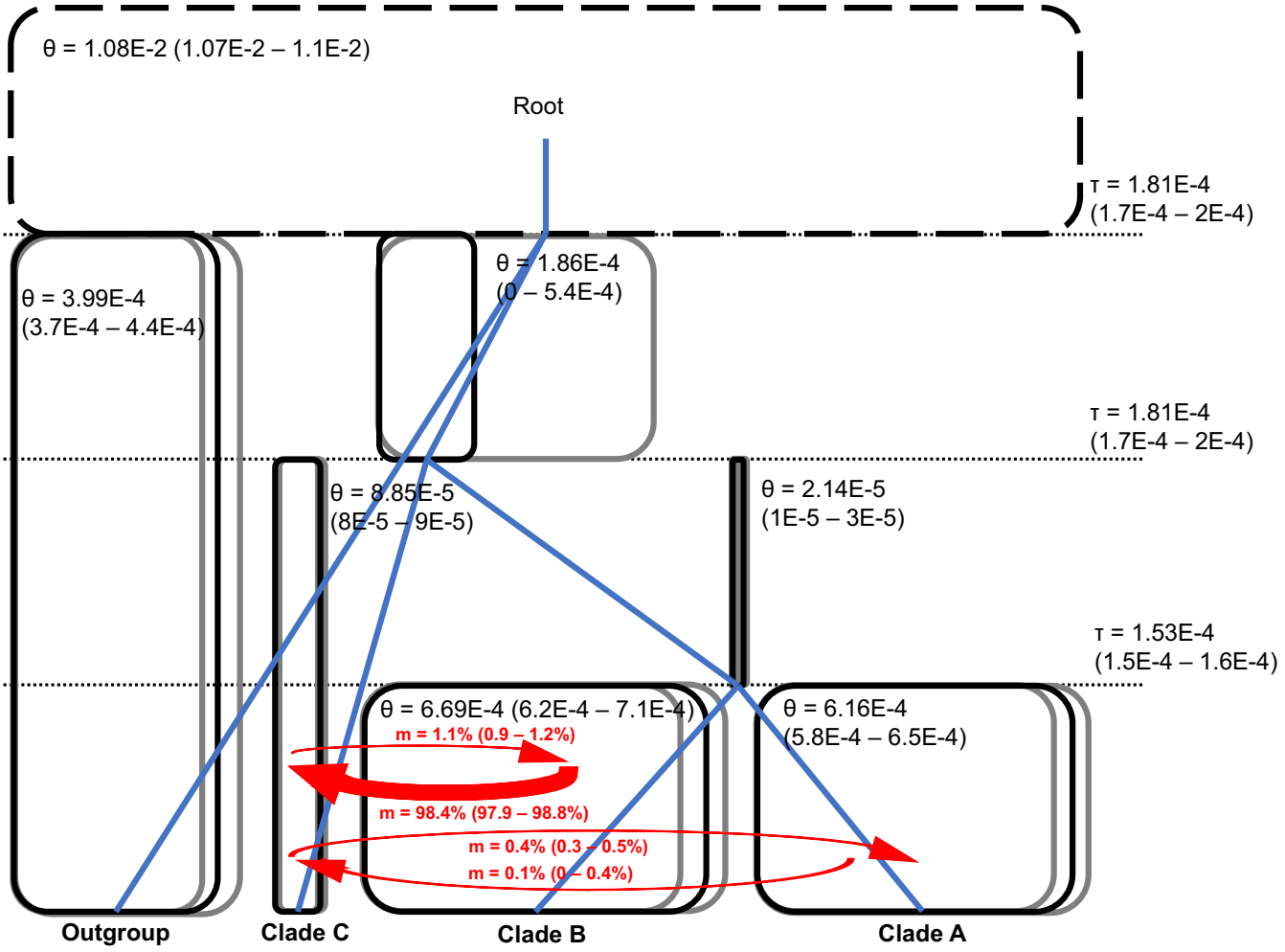

FIGURE 4 Demographic history of *Carex furva* and *C. lucennoiberica* as inferred by G-PhoCS analysis. Clades correspond with those in Figure 2, where clade A contains only *C. lucennoiberica* samples, clade B gathers *C. lucennoiberica* plus hybrid individuals with haplotypes H4 and H7, and clade C includes a *C. furva* individual plus a hybrid individual with haplotype H3. Boxes indicated sampled and ancestral populations, and blue line shows the topology of the phylogeny. Relative population sizes (θ) are indicated including the 95% highest posterior density (HPD) interval in parenthesis. Width of the boxes is proportional to those population sizes except for the root, and grey boxes indicate the 95% HPD intervals; relative divergence times of clades (τ) are also shown (95% HPD in parenthesis), where the most recent time is on the bottom of the figure; migration bands (m) are represented with red arrows, where the main migration route is indicated with a wider arrow. Percentage of migration detected for each direction is specified, including 95% HPD interval

Guerra-Cárdenas, Lye, & Luceño, 2011), and a number of other species endemic to Iberian alpine habitats such as *Campanula herminii* (Sáez & Aldasoro, 2001), *Gentiana boryi* (Renobales, 2012), *Linaria elegans* (Fernández-Mazuecos & Vargas, 2013) or *Senecio boissieri* (Peredo et al., 2009). Such restriction of gene flow among mountain refugia could be a precursor to speciation. *Carex furva–C. lucennoiberica* clade may be thought of as either one species in the midst of speciation or as two very young species with an intermediate morphotype. Nevertheless, these lineages satisfy the evolutionary species criteria (they are both lineages with their own evolutionary roles and tendencies; De Queiroz, 2007), and they are diagnosable both morphologically and genetically (Maguilla & Escudero, 2016; but see also Figure 1). Allopatry seems to have driven differentiation of *C. furva* and *C. lucennoiberica*.

4.2 | Secondary contacts and speciation during the Quaternary

Climatic oscillations during the Quaternary shaped the biodiversity of Europe by forcing species to move along altitudinal and latitudinal gradients, driving diversification and genetic differentiation of these species in glacial refugia (Hewitt, 2004). Although climatic changes during the Pleistocene have been shown to decrease speciation rates in some organisms (Turgeon, Stoks, Thum, Brown, & Mcpeek, 2005), the effect of glaciations in isolating populations within species had a positive effect on speciation rates in many groups of organisms (e.g., Bennett, 2004; Good-Avila, Souza, Gaut, & Eguiarte, 2006; Zink, Klicka, & Barber, 2004). Alternating cycles of population fragmentation and expansion during the Pleistocene provided opportunities for

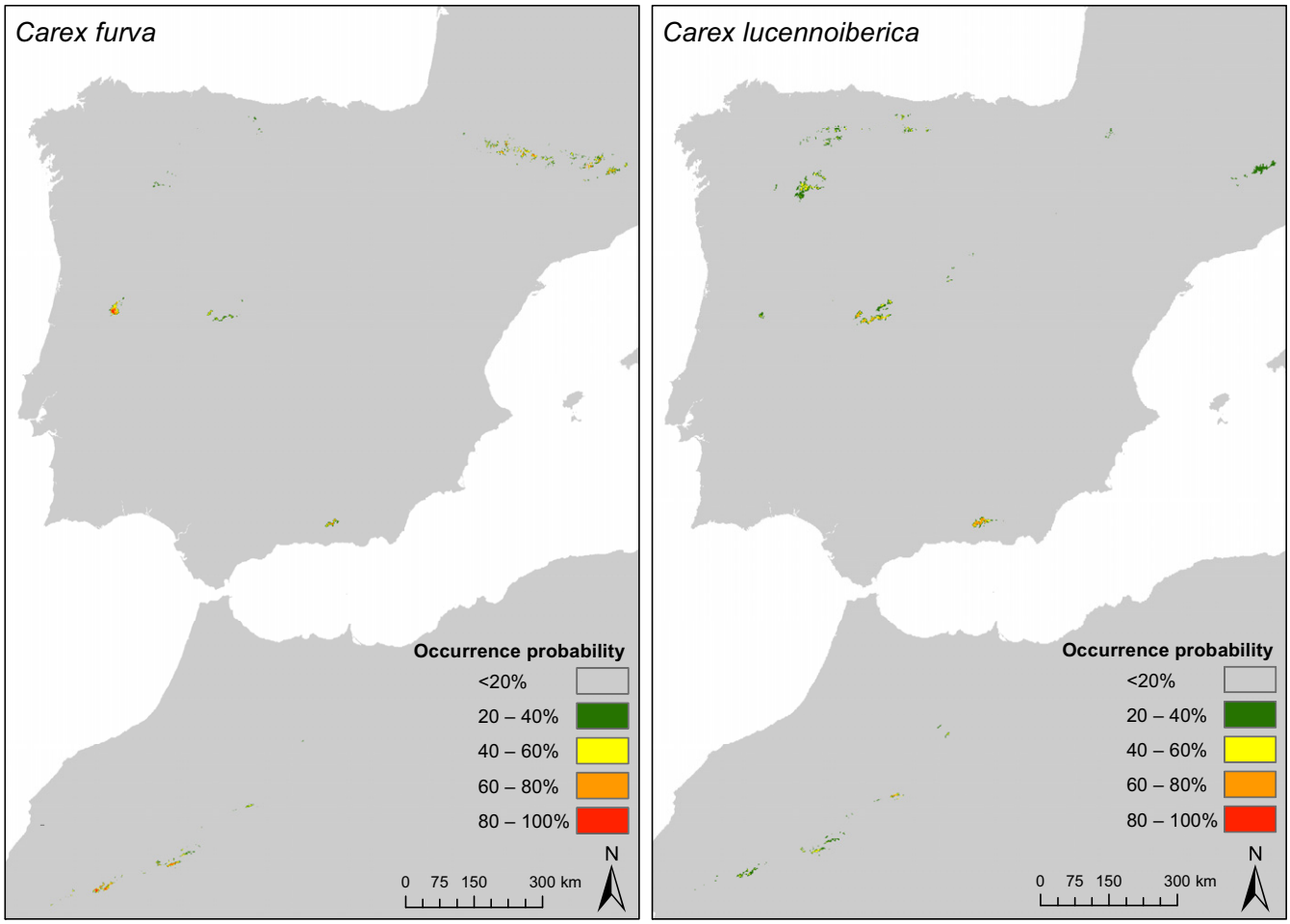

FIGURE 5 Results of species distribution modelling in MAXENT v.3.3 under current climatic conditions, showing average potential distribution (=average niche suitability) of *Carex furva* and *C. lucennoiberica*

demographic fluctuations and population divergence as well as episodes of secondary contact or hybridization (Avise, 2000). The origin of *C. furva–C. lucennoiberica*, ca. 1.98 Ma (Maguilla et al., under review) suggests that a broader and more continuous distribution of the ancestral species during colder periods was followed by disjunction among populations that became isolated in high mountains after glaciations of the Pleistocene (Figure 1). This pattern of range expansions and contractions is congruent with our projections to the LGM and LIG (Figure 6); both species present the widest potential distributions during glacial periods (see projection to LGM). Differentiation between the species identified in this study (Figure 1) was thus most likely a consequence of allopatry during the warmest periods. The projections to the LGM indicate that the distribution of *C. furva* and *C. lucennoiberica* was wider but not continuous, at least during the LGM. Nevertheless, a more widespread ancestral distribution could have facilitated gene flow among populations by long-distance dispersal (LDD). *Carex furva* and *C. lucennoiberica* suffered distribution-range contractions and geographic isolation during warm periods, as has been reported in at least one other plant species (Kropf, Comes, & Kadereit, 2006). This cycle of range expansions and contractions would explain the finding of haplotypes intermediate between *C. furva* and *C. lucennoiberica* in the southern Iberian Peninsula (Figure 1). Based on RAD-seq analyses (Figures 2 and 3), the individuals of the intermediate population with intermediate haplotypes (H4 and H7) are more closely related to *C. lucennoiberica* than to *C. furva*. This suggests that during secondary contact, the dominant direction of introgression has been from the more widespread species (*C. lucennoiberica*) to the more narrowly distributed species (*C. furva*). An alternative scenario would be the existence of single refugium of the ancestral species and diversification in Sierra Nevada followed by colonization of northern latitudes by *C. lucennoiberica*. However, two lines of evidence suggest at least a second refugium in the Sistema Central (in the central Iberian Peninsula): (i) the highest diversity of haplotypes (H1, H2, H5 and H7) is found in Sistema Central, and these four haplotypes are exclusive of *C. lucennoiberica* (none of them are found in *C. furva* or the intermediate individuals), and (ii) none of these four haplotypes is found in Sierra Nevada. As stated before, this evidence suggests the existence of at least two refugia disjunct from each other. Thus, we cannot fully discard the single refugium hypothesis in the Southern Iberian Peninsula and later dispersion to northern latitudes. Nevertheless, our results suggest that this hypothesis is less plausible.

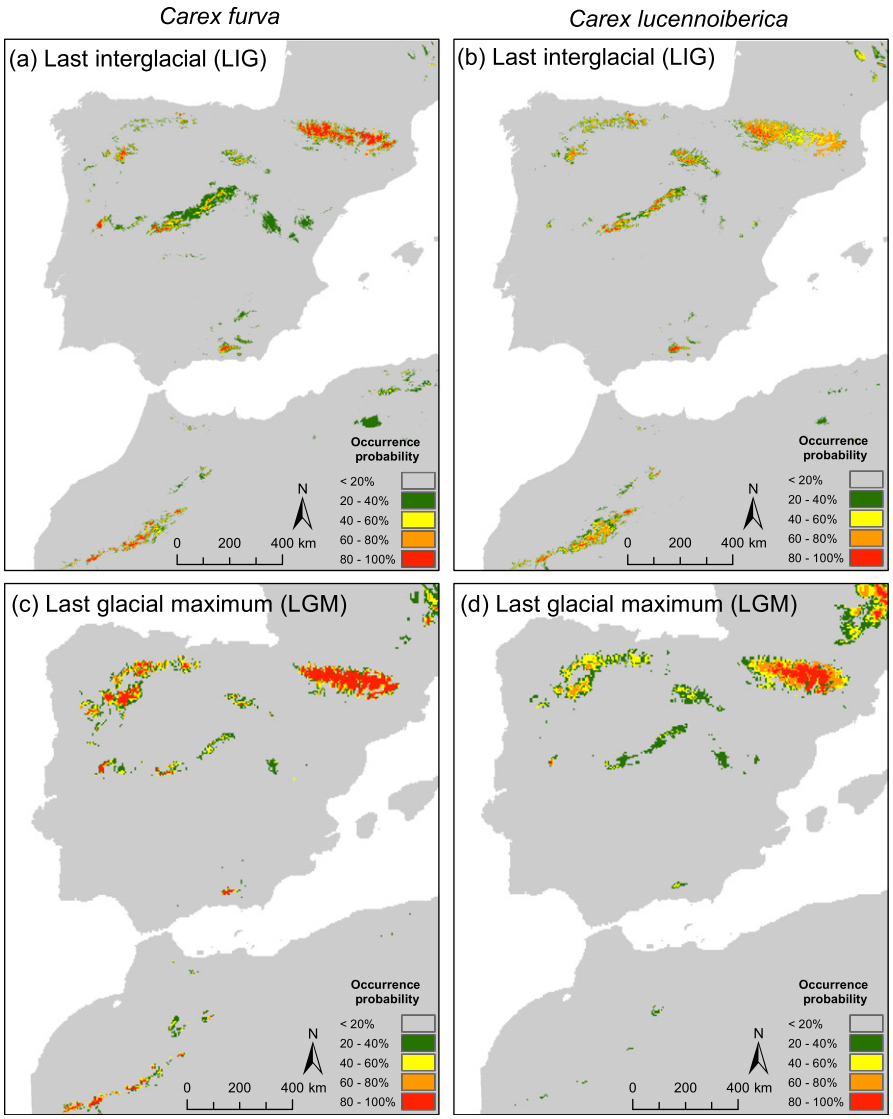

FIGURE 6 Results of the species distribution modelling in MAXENT v.3.3 projected to past climatic conditions, showing the average distribution (=average niche suitability) of *Carex furva* and *C. lucennoiberica* during the last interglacial period (LIG; ca 120–140 kyr bp) and the last glacial maximum (LGM; ca 21 kyr bp)

Based on partitioned *D*-statistic tests (Figure 2; Table S2), the most plausible pattern of secondary contact is from central populations of *C. lucennoiberica* to the south, which is also supported by the G-PhoCS analysis (Figure 4). These secondary contact events might be due to recent LDD. However, the lack of any haplotype typical of *C. lucennoiberica* (H1, H2, H5 and H6) and the presence of intermediate haplotypes (H4 and H7) in the south make recent long-distance dispersal very unlikely (Figure 1). In addition, the finding of secondary patterns of introgression from northern populations of *C. lucennoiberica* to the south and south-to-north introgression (Figures 2 and 4; Table S2) makes sense in the light of the history of range expansions and contractions inferred under alternating glacial and interglacial cycles during the Pleistocene (Ikeda, Carlsen, Fujii, Brochmann, & Setoguchi, 2012) and admixture among populations of both species in lower altitudes during colder periods. These population expansions and contractions appear to be a common pattern in mountain plant species in the Iberian Peninsula (Fernández-Mazuecos & Vargas, 2013; Robledo-Arnuncio, Collada, Alía, & Gil, 2005). This does not rule out the possibility that LDD may have contributed to gene flow between *C. furva* and *C. lucennoiberica*, which were not fully continuous during glacial periods. LDD is not uncommon in the Cyperaceae (Viljoen et al., 2013), including *Carex* (e.g., Villaverde, Escudero, Luceño, & Martín-Bravo, 2015; Villaverde, Escudero, Martín-Bravo et al., 2015). This fact notwithstanding, our study strongly supports asymmetrical introgression during periods of secondary contact due to range expansion and LDD as the dominant cause of gene flow between *C. furva* and *C. lucennoiberica*.

4.3 | Speciation with gene flow vs. speciation reversal

While moderate levels of gene flow can prevent speciation or divergence among populations (Bolnick & Nosil, 2007; Räsänen & Hendry, 2008), speciation is possible even in the face of limited dispersal and gene flow between populations (Runemark et al., 2012). Gene flow or historical hybridization has been relatively common among species during the Quaternary (Cronn & Wendel, 2003; Pelser et al., 2010), and it can occur in both endemic and widespread species (Ikeda

et al., 2012) without eroding species boundaries. However, speciation reversal in the face of gene flow has been demonstrated in animals (e.g., Bhat et al., 2014; Seehausen, 2006; Taylor et al., 2005; Vonlanthen et al., 2012; Webb, Marzluff, & Omland, 2011) and is typically shown to erode incipient species boundaries in few generations (Taylor et al., 2005). Speciation reversal requires the rate of gene flow between species to exceed the rate of gene flow among individuals within the species, which may be due to a change in ecological conditions that favours contact among species (Seehausen, 2006).

While there has been gene flow between *C. furva* and *C. lucennoiberica*, the strong morphological, genetic and ecological coherence of each species suggests that interspecific gene flow is weaker than gene flow within the species. This is not, therefore, an example of speciation reversal (Turner, 2002). *Carex furva* and *C. lucennoiberica* have maintained morphological and phylogenetic distinctiveness in spite of historical gene flow among them, but also despite climatic and ecological oscillations during the Quaternary.

We conclude that the species diverged in allopatry in at least two different interglacial refugia and that multiple instances of secondary contact during glacial periods of the Quaternary have been insufficient to reverse speciation.

ACKNOWLEDGEMENTS

We thank BABY, BM, DAO, H, M, MHA, RSA, UPOS and WTU herbaria and their staff for allowing us to study their collections and get samples of the specimens. We also thank editor L. Rieseberg and three anonymous reviewers for their comments, which improved an earlier version of this manuscript, A. Silva (Centro de Interpretaçao da Serra da Estrela, Portugal) and the staff of Sierra de Guadarrama and Sierra Nevada National Parks (Spain) for providing collecting permits, F. Fernández-González (University of Castilla la Mancha, Spain) for providing helpful information to find *C. lucennoiberica* from Sierra de Guadarrama (Spain), M. Hahn (The Morton Arboretum, Lisle, IL, USA), F.J. Fernández and M.Míguez (UPO) for technical support, and J.M.G. Cobos and T.Villaverde (UPO) for participating in collecting trips. This work was supported through a FPU-fellowship to E.M. (AP2012-2189) from the Spanish Government; a Synthesys grant to E.M. (GB-TAF-2523) by the European Community Research Infrastructures Program (European Comission); research grants to M.L., E.M. and M.E. funded by the Spanish Government (CGL2012-38744, CGL2016-77401-P) and Junta de Andalucía (RNM2763); and National Science Foundation grant 1255901 to A.L.H.

DATA ACCESSIBILITY

Obtained DNA sequences for cpDNA *atp*I-*atp*H and *psb*A-*trn*H are available in NCBI GenBank with Accession nos. KU997965 to KU998098 for *atp*I-*atp*H and KU998099 to KU998232 for *psb*A-*trn*H.

Obtained RAD-seq data are available on the NCBI SRA archive SRP073698 under BioProject Accession no. PRJNA319297.

AUTHOR CONTRIBUTIONS

All authors designed and conceived the study. E.M. performed the laboratory and fieldwork, generated the data and drafted the article. E.M., A.L.H. and M.E. analysed the data. All authors interpreted and discussed the data and wrote the manuscript.

ORCID

Enrique Maguilla http://orcid.org/0000-0002-8245-3024
Marcial Escudero https://orcid.org/0000-0002-2541-5427
Andrew L. Hipp https://orcid.org/0000-0002-1241-9904
Modesto Luceño https://orcid.org/0000-0002-0336-4083

REFERENCES

Abbott, R., Albach, D., Ansell, S., Arntzen, J. W., Baird, S. J. E., Bierne, N., … Zinner, D. (2013). Hybridization and speciation. *Journal of Evolutionary Biology*, *26*, 229–246.

Aberer, A. J., Kobert, K., & Stamatakis, A. (2014). ExaBayes: Massively parallel bayesian tree inference for the whole-genome era. *Molecular Biology and Evolution*, *31*, 2553–2556.

Akaike, H. (1974). A new look at the statistical model identification. *IEEE Transactions on Automatic Control*, *19*, 716–723.

Avise, J. C. (2000). *Phylogeography: The history and formation of species*. Cambridge, MA: Harvard University Press.

Baird, N. A., Etter, P. D., Atwood, T. S., Currey, M. C., Shiver, A. L., Lewis, Z. A., … Johnson, E. A. (2008). Rapid SNP discovery and genetic mapping using sequenced RAD markers. *PLoS ONE*, *3*, e3376.

Bennett, K. D. (2004). Continuing the debate on the role of Quaternary environmental change for macroevolution. *Philosophical Transactions of the Royal Society of London. Series B, Biological Sciences*, *359*, 295–303.

Bennett, K., Tzedakis, P., & Willis, K. (1991). Quaternary refugia of North European trees. *Journal of Biogeography*, *18*, 103–115.

Bhat, S., Amundsen, P.-A., Knudsen, R., Gjelland, K. Ø., Fevolden, S.-E., Bernatchez, L., & Præbel, K. (2014). Speciation reversal in European Whitefish (*Coregonus lavaretus* (L.)) caused by competitor invasion. *PLoS ONE*, *9*, e91208.

Bolnick, D. I., & Nosil, P. (2007). Natural selection in populations subject to a migration load. *Evolution*, *61*, 2229–2243.

Brochmann, C., Gabrielsen, T. M., & Nordal, I. (2003). Glacial survival or tabula rasa? The history of North Atlantic biota revisited. *Taxon*, *52*, 417–450.

Brummitt, R. K. (2001). World geographical scheme for recording plant distributions, 2nd edition. *Hunt institute for botanical documentation* (pp. 1–137). Pittsburgh: Carnegie Mellon University.

Cayouette, J., & Catling, P. (1992). Hybridization in the genus *Carex* with special reference to North America. *The Botanical Review*, *58*, 351–438.

Clement, M., Posada, D., & Crandall, K. A. (2000). TCS: A computer program to estimate gene genealogies. *Molecular Ecology*, *9*, 1657–1659.

Cronn, R., & Wendel, J. F. (2003). Cryptic trysts, genomic merges, and plant speciation. *New Phytologist*, *161*, 133–142.

Darriba, D., Taboada, G. L., Doallo, R., & Posada, D. (2012). jModelTest 2: More models, new heuristics and parallel computing. *Nature Methods*, *9*, 772.

De Queiroz, K. (2007). Species concepts and species delimitation. *Systematic Botany*, *56*, 879–886.

Durand, E. Y., Patterson, N., Reich, D., & Slatkin, M. (2011). Testing for ancient admixture between closely related populations. *Molecular Biology and Evolution*, *28*, 2239–2252.

Eaton, D. A. R. (2014). PyRAD: Assembly of de novo RADseq loci for phylogenetic analyses. *Bioinformatics*, *30*, 1844–1849.

Eaton, D. A. R., Hipp, A. L., González-Rodríguez, A., & Cavender-Bares, J. (2015). Historical introgression among the American live oaks and the comparative nature of tests for introgression. *Evolution*, *69*, 2587–2601.

Eaton, D. A. R., & Ree, R. H. (2013). Inferring phylogeny and introgression using RADseq data: An example from flowering plants (*Pedicularis*: Orobanchaceae). *Systematic Biology*, *62*, 689–706.

Edgar, R. C. (2004). MUSCLE: A multiple sequence alignment method with reduced time and space complexity. *BMC Bioinformatics*, *5*, 113.

Escudero, M., Eaton, D. A. R., Hahn, M., & Hipp, A. L. (2014). Genotyping-by-sequencing as a tool to infer phylogeny and ancestral hybridization: A case study in *Carex* (Cyperaceae). *Molecular Phylogenetics and Evolution*, *79*, 359–367.

Escudero, M., & Hipp, A. L. (2013). Shifts in diversification rates and clade ages explain species richness in higher-level sedge taxa (Cyperaceae). *American Journal of Botany*, *100*, 2403–2411.

Escudero, M., Hipp, A. L., Waterway, M. J., & Valente, L. M. (2012). Diversification rates and chromosome evolution in the most diverse angiosperm genus of the temperate zone (*Carex*, Cyperaceae). *Molecular Phylogenetics and Evolution*, *63*, 650–655.

Escudero, M., & Luceño, M. (2009). Systematics and evolution of *Carex* sects. *Spirostachyae* and *Elatae* (Cyperaceae). *Plant Systematics and Evolution*, *279*, 163–189.

Felsenstein, J. (1976). The theoretical population genetics of variable selection and migration. *Annual Review of Genetics*, *10*, 253–280.

Fernández-Mazuecos, M., & Vargas, P. (2013). Congruence between distribution modelling and phylogeographical analyses reveals Quaternary survival of a toadflax species (*Linaria elegans*) in oceanic climate areas of a mountain ring range. *The New Phytologist*, *198*, 1274–1289.

Fick, S. E., & Hijmans, R. J. (2017). WorldClim 2: New 1-km spatial resolution climate surfaces for global land areas. *International Journal of Climatology*. http://org.doi:10.1002/joc.5086

Fitzpatrick, B. M. F., Ryan, M. E. R., Johnson, J. R. J., Corush, J. C., & Carter, E. T. C. (2015). Hybridization and the species problem in conservation. *Current Zoology*, *61*, 206–216.

Ford, C. S., Ayres, K. L., Toomey, N., Haider, N., Van Alphen Stahl, J., Kelly, L. J., … Wilkinson, M. J. (2009). Selection of candidate coding DNA barcoding regions for use on land plants. *Botanical Journal of the Linnean Society*, *159*, 1–11.

García-Ramos, G., & Kirkpatrick, M. (1997). Genetic models of adaptation and gene flow in peripheral populations. *Evolution*, *51*, 21–28.

Gehrke, B., Martín-Bravo, S., Muasya, M., & Luceño, M. (2010). Monophyly, phylogenetic position and the role of hybridization in *Schoenoxiphium* Nees (*Cariceae*, Cyperaceae). *Molecular Phylogenetics and Evolution*, *56*, 380–392.

Gent, P. R., Danabasoglu, G., Donner, L. J., Holland, M. M., Hunke, E. C., Jayne, S. R., … Zhang, M. (2011). The community climate system model version 4. *Journal of Climate*, *24*, 4973–4991.

Giorgetta, M. A., Jungclaus, J. H., Reick, C. H., Legutke, S., Bader, J., Böttinger, M., … Stevens, B. (2013). Climate and carbon cycle changes from 1850 to 2100 in MPI-ESM simulations for the coupled model intercomparison project phase 5. *Journal of Advances in Modeling Earth Systems*, *5*, 572–597.

Global Carex Group (2015). Making *Carex* monophyletic (Cyperaceae, tribe *Cariceae*): A new broader circumscription. *Botanical Journal of the Linnean Society*, *179*, 1–42.

Goloboff, P. A., Farris, J. S., & Nixon, K. C. (2008). TNT, a free program for phylogenetic analysis. *Cladistics*, *24*, 774–786.

Good-Avila, S. V., Souza, V., Gaut, B. S., & Eguiarte, L. E. (2006). Timing and rate of speciation in *Agave* (Agavaceae). *Proceedings of the National Academy of Sciences of the United States of America*, *103*, 9124–9129.

Green, R. E., Krause, J., Briggs, A. W., Maricic, T., Stenzel, U., Kircher, M., … Pääbo, S. (2010). A draft sequence of the Neandertal genome. *Science*, *328*, 710–722.

Gronau, I., Hubisz, M. J., Gulko, B., Danko, C. G., & Siepel, A. (2011). Bayesian inference of ancient human demography from individual genome sequences. *Nature Genetics*, *43*, 1031–1034.

Harvey, M. G., Seeholzer, G. F., Smith, B. T., Rabosky, D. L., Cuervo, A. M., & Brumfield, R. T. (2017). Positive association between population genetic differentiation and speciation rates in New World birds. *Proceedings of the National Academy of Sciences of the United States of America*, *114*, 6328–6333.

Hedrick, P. W. (2013). Adaptive introgression in animals: Examples and comparison to new mutation and standing variation as sources of adaptive variation. *Molecular Ecology*, *22*, 4606–4618.

Hedrick, P. W., & Fredrickson, R. (2010). Genetic rescue guidelines with examples from Mexican wolves and Florida panthers. *Conservation Genetics*, *11*, 615–626.

Hendry, A. P., Day, T., & Taylor, E. B. (2001). Population mixing and the adaptive divergence of quantitative traits in discrete populations: A theoretical framework for empirical tests. *Evolution*, *55*, 459–466.

Hendry, A. P., & Taylor, E. B. (2004). How much of the variation in adaptive divergence can be explained by gene flow? An evaluation using lake-stream stickleback pairs. *Evolution*, *58*, 2319–2331.

Hewitt, G. M. (2000). The genetic legacy of the Quaternary ice ages. *Nature*, *405*, 907–913.

Hewitt, G. M. (2004). Genetic consequences of climatic oscillations in the Quaternary. *Philosophical Transactions of the Royal Society B: Biological Sciences*, *359*, 183–195.

Hipp, A. L. (2014). *RADami: R package for phylogenetic analysis of RADseq data*. R package version 1.0-3. Retrieved from http://CRAN.R–project.org/package=RADami

Hipp, A. L., Eaton, D. A. R., Cavender-Bares, J., Fitzek, E., Nipper, R., & Manos, P. S. (2014). A framework phylogeny of the American oak clade based on sequenced RAD data. *PLoS ONE*, *9*, e93975.

Ikeda, H., Carlsen, T., Fujii, N., Brochmann, C., & Setoguchi, H. (2012). Pleistocene climatic oscillations and the speciation history of an alpine endemic and a widespread arctic-alpine plant. *New Phytologist*, *194*, 583–594.

Jiménez-Mejías, P., Escudero, M., Guerra-Cárdenas, S., Lye, K. A., & Luceño, M. (2011). Taxonomic delimitation and drivers of speciation in the Ibero-North African *Carex* sect. *Phacocystis* river-shore group (Cyperaceae). *American Journal of Botany*, *98*, 1855–1867.

Jiménez-Mejías, P., Luceño, M., & Martín-Bravo, S. (2014). Species boundaries within the Southwest Old World populations of the *Carex flava* group (Cyperaceae). *Systematic Botany*, *39*, 117–131.

Jiménez-Mejías, P., Martín-Bravo, S., & Luceño, M. (2012). Systematics and taxonomy of *Carex* sect. *Ceratocystis* (Cyperaceae) in Europe: A molecular and cytogenetic approach. *Systematic Botany*, *37*, 382–398.

Jombart, T. (2008). adegenet: A R package for the multivariate analysis of genetic markers. *Bioinformatics*, *24*, 1403–1405.

Jombart, T., Devillard, S. & Balloux, F., (2010). Discriminant analysis of principal components: A new method for the analysis of genetically structured populations. *BMC Genetics*, *11*, 94.

Judd, W. S., Campbell, C. S., Kellogg, E. A., Stevens, P. F., & Donoghe, M. J. (2007). *Plant systematics: A phylogenetic approach*, 3rd ed. Sunderland. Kluge: Sinauer Associates Inc.

Kropf, M., Comes, H. P., & Kadereit, J. W. (2006). Long-distance dispersal vs vicariance: The origin and genetic diversity of alpine plants in the Spanish Sierra Nevada. *New Phytologist*, *172*, 169–184.

Lamichhaney, S., Berglund, J., Almén, M. S., Maqbool, K., Grabherr, M., Martínez-Barrio, A., … Andersson, L. (2015). Evolution of Darwin's finches and their beaks revealed by genome sequencing. *Nature*, *518*, 371–375.

Latch, E. K., Harveson, L. A., King, J. S., Hobson, M. D., & Rhodes, O. E. Jr (2006). Assessing hybridization in wildlife populations using

molecular markers: A case study in wild turkeys. *Journal of Wildlife Management*, *70*, 485–492.

Lewontin, R. C., & Birch, L. C. (1966). Hybridization as a source of variation for adaptation to new environments. *Evolution*, *20*, 315–336.

Luceño, M. (1986). Estudios en el género *Carex*. I. Sección *Canescentes* (Fries) Christ.: *C. furva* Webb Y *C. lachenalii* Schkuhr. *Anales del Jardín Botánico de Madrid*, *42*, 427–440.

Luceño, M. (2008). *Carex* L. In S. Castroviejo, M. Luceño, A. Galan, et al. (Eds.), *Flora iberica* (pp. 146–151). Madrid: Real Jardin Botanico, CSIC.

Maguilla, E., & Escudero, M. (2016). Cryptic species due to hybridization: A combined approach to describe a new species (*Carex*: Cyperaceae). *PLoS ONE*, *11*, e0166949.

Maguilla, E., Escudero, M., Waterway, M. J., Hipp, A. L., & Luceño, M. (2015). Phylogeny, systematics, and trait evolution of *Carex* section *Glareosae*. *American Journal of Botany*, *102*, 1128–1144.

Mallet, J. (2005). Hybridization as an invasion of the genome. *Trends in Ecology and Evolution*, *20*, 229–237.

Marques, I., Draper, D., Riofrío, L., & Naranjo, C. (2014). Multiple hybridization events, polyploidy and low postmating isolation entangle the evolution of neotropical species of *Epidendrum* (Orchidaceae). *BMC Evolutionary Biology*, *14*, 20.

McVay, J. D., Hipp, A. L., & Manos, P. S. (2017). A genetic legacy of introgression confounds phylogeny and biogeography in oaks. *Proceedings of the Royal Society of London B*, *284*, 20170300.

Neuditschko, M., Khatkar, M. S., & Raadsma, H. W. (2012). NetView: A high-definition network-visualization approach to detect fine-scale population structures from genome-wide patterns of variation. *PLoS ONE*, *7*, e48375.

Nogués-Bravo, D. (2009). Predicting the past distribution of species climatic niches. *Global Ecology and Biogeography*, *18*, 521–531.

Oliveira, R., Godinho, R., Randi, E., & Alves, P. C. (2008). Hybridization versus conservation: Are domestic cats threatening the genetic integrity of wildcats (*Felis silvestris silvestris*) in Iberian Peninsula? *Philosophical Transactions of the Royal Society of London. Series B, Biological Sciences*, *363*, 2953–2961.

Otto-Bliesner, B. L., Marshall, S. J., Overpeck, J. T., Miller, G. H., & Hu, A. (2006). Simulating Arctic climate warmth and icefield retreat in the last interglaciation. *Science*, *311*, 1751–1753.

Pardo-Diaz, C., Salazar, C., Baxter, S. W., Merot, C., Figueiredo-Ready, W., Joron, M., … Jiggins, C. D. (2012). Adaptive introgression across species boundaries in *Heliconius* butterflies. *PLoS Genetics*, *8*, e1002752.

Pauli, H., Gottfried, M., & Grabherr, G. (1996). Effects of climate change on mountain ecosystems - upward shifting of alpine plants. *World Resource Review*, *8*, 382–390.

Pelser, P. B., Kennedy, A. H., Tepe, E. J., Shidler, J. B., Nordenstam, B., Kadereit, J. W., & Watson, L. E. (2010). Patterns and causes of incongruence between plastid and nuclear *Senecioneae* (Asteraceae) phylogenies. *American Journal of Botany*, *97*, 856–873.

Peredo, E. L., Revilla, M. A., Jiménez-Alfaro, B., Bueno, A., Prieto, A. F. J., & Abbott, R. J. (2009). Historical biogeography of a disjunctly distributed, Spanish alpine plant, *Senecio boissieri* (Asteraceae). *Taxon*, *58*, 883–892.

Petit, R. J., Aguinagalde, I., de Beaulieu, J.-L., Bittkau, C., Brewer, S., Cheddadi, R., … Vendramin, G. G. (2003). Glacial refugia: Hotspots but not melting pots of genetic diversity. *Science*, *300*, 1563–1565.

Phillips, S. J., Anderson, R. P., & Schapire, R. E. (2006). Maximum entropy modeling of species geographic distributions. *Ecological Modelling*, *190*, 231–259.

R Core Team (2015). *R: A language and environment for statistical computing*. Vienna, Austria: R Foundation for Statistical Computing.

Rambaut, A., & Drummond, A. J. (2014). *Tracer v1.6*. Retrieved from http://beast.bio.ed.ac.uk/Tracer

Räsänen, K., & Hendry, A. P. (2008). Disentangling interactions between adaptive divergence and gene flow when ecology drives diversification. *Ecology Letters*, *11*, 624–636.

Ree, R. H., & Hipp, A. L. (2015). Inferring phylogenetic history from restriction site associated DNA (RADseq). In E. Hörandl, & M. Appelhans (Eds.), *Next-generation sequencing in plant systematics* (pp. 181–204). Koenigstein: Koeltz Scientific Books.

Renobales, G. (2012). *Gentiana* L. In S. Talavera, C. Andrés, M. Arista, et al. (Eds.), *Flora iberica, vol. XI* (pp. 5–35). Madrid (Spain): CSIC.

Robledo-Arnuncio, J. J., Collada, C., Alía, R., & Gil, L. (2005). Genetic structure of montane isolates of *Pinus sylvestris* L. in a Mediterranean refugial area. *Journal of Biogeography*, *32*, 595–605.

Ronquist, F., Teslenko, M., van der Mark, P., Ayres, D. L., Darling, A., Höhna, S., … Huelsenbeck, J. P. (2012). MrBayes 3.2: Efficient Bayesian phylogenetic inference and model choice across a large model space. *Systematic Biology*, *61*, 539–542.

Runemark, A., Hey, J., Hansson, B., & Svensson, E. I. (2012). Vicariance divergence and gene flow among islet populations of an endemic lizard. *Molecular Ecology*, *21*, 117–129.

Sáez, L., & Aldasoro, J. J. (2001). *Campanula* L. In J. Paiva, F. Sales, I. C. Hedge, et al. (Eds.), *Flora iberica, vol. XIV* (pp. 105–136). Madrid (Spain): CSIC.

Sang, T., Crawford, D., & Stuessy, T. (1997). Chloroplast DNA phylogeny, reticulate evolution, and biogeography of *Paeonia* (Paeoniaceae). *American Journal of Botany*, *84*, 1120.

Seehausen, O. (2006). Sympatric speciation: Why the controversy? *Current Biology*, *16*, R333–R334.

Shaw, J., Lickey, E. B., Beck, J. T., Farmer, S. B., Liu, W., Miller, J., … Small, R. L. (2005). The tortoise and the hare II: Relative utility of 21 noncoding chloroplast DNA sequences for phylogenetic analysis. *American Journal of Botany*, *92*, 142–166.

Shaw, J., Lickey, E. B., Schilling, E. E., & Small, R. L. (2007). Comparison of whole chloroplast genome sequences to choose noncoding regions for phylogenetic studies in angiosperms: The tortoise and the hare III. *American Journal of Botany*, *94*, 275–288.

Simmons, M., & Ochoterena, H. (2000). Gaps as characters in sequence-based phylogenetic analyses. *Systematic Biology*, *49*, 369–381.

Soltis, P. S. (2013). Hybridization, speciation and novelty. *Journal of Evolutionary Biology*, *26*, 291–293.

Soltis, P. S., & Soltis, D. E. (2009). The role of hybridization in plant speciation. *Annual Review of Plant Biology*, *60*, 561–588.

Stamatakis, A., Hoover, P., & Rougemont, J. (2008). A rapid bootstrap algorithm for the RAxML web servers. *Systematic Biology*, *57*, 758–771.

Stankowski, S., & Streisfeld, M. A. (2015). Introgressive hybridization facilitates adaptive divergence in a recent radiation of monkeyflowers. *Proceedings of the Royal Society of London B*, *282*, 20151666.

Steinig, E. J., Neuditschko, M., Khatkar, M. S., Raadsma, H. W., & Zenger, K. R. (2016). NetView p : A network visualization tool to unravel complex population structure using genome-wide SNPs. *Molecular Ecology Resources*, *16*, 216–227.

Taberlet, P., Fumagalli, L., Wust-Saucy, A. G., & Cosson, J. F. (1998). Comparative phylogeography and postglacial colonization routes in Europe. *Molecular Ecology*, *7*, 453–464.

Tate, J. A., & Simpson, B. B. (2003). Paraphyly of *Tarasa* (Malvaceae) and diverse origins of the polyploid species. *Systematic Botany*, *28*, 723–737.

Taylor, E. B., Boughman, J. W., Groenenboom, M., Sniatynski, M., Schluter, D., & Gow, J. L. (2005). Speciation in reverse: Morphological and genetic evidence of the collapse of a three-spined stickleback (*Gasterosteus aculeatus*) species pair. *Molecular Ecology*, *15*, 343–355.

Templeton, A. R., Crandall, K. A., & Sing, C. F. (1992). A cladistic analysis of phenotypic associations with haplotypes inferred from restriction endonuclease mapping and DNA sequence data. III. Cladogram estimation. *Genetics*, *132*, 619–633.

The Heliconius Genome Consortium (2012). Butterfly genome reveals promiscuous exchange of mimicry adaptations among species. *Nature*, *487*, 94–98.

Thiers, B. (2015). Index Herbariorum: A global directory of public herbaria and associated staff. *New York Botanical Garden's Virtual Herbarium*. Retrieved from http://sweetgum.nybg.org/ih/

Tribsch, A., & Schönswetter, P. (2003). Patterns of endemism and comparative phylogeography confirm palaeoenvironmental evidence for Pleistocene refugia in the Eastern Alps. *Taxon*, *52*, 477–497.

Turgeon, J., Stoks, R., Thum, R. A., Brown, J. M., & Mcpeek, M. A. (2005). Simultaneous quaternary radiations of three damselfly clades across the Holarctic. *The American Naturalist*, *165*, E78–E107.

Turner, G. F. (2002). Parallel speciation, despeciation and respeciation: Implications for species definition. *Fish and Fisheries*, *3*, 225–229.

Van Andel, T. H., & Tzedakis, P. C. (1996). Palaeolithic landscapes of Europe and environs, 150,000–25,000 years ago: An overview. *Quaternary Science Reviews*, *15*, 481–500.

Van Valen, L. (1976). Ecological species, multispecies, and oaks. *Taxon*, *25*, 233–239.

Vargas, P. (2003). Molecular evidence for multiple diversification patterns of alpine plants in Mediterranean Europe. *Taxon*, *52*, 463–476.

Viljoen, J. A., Muasya, M., Barrett, R. L., Bruhl, J. J., Gibbs, A. K., Slingsby, J. A., … Verboom, G. A. (2013). Radiation and repeated transoceanic dispersal of *Schoeneae* (Cyperaceae) through the southern hemisphere. *American Journal of Botany*, *100*, 2494–2508.

Villaverde, T., Escudero, M., Luceño, M., & Martín-Bravo, S. (2015). Long-distance dispersal during the middle-late Pleistocene explains the bipolar disjunction of *Carex maritima* (Cyperaceae). *Journal of Biogeography*, *42*, 1820–1831.

Villaverde, T., Escudero, M., Martín-Bravo, S., Bruederle, L. P., Luceño, M., & Starr, J. R. (2015). Direct long-distance dispersal best explains the bipolar distribution of *Carex arctogena* (*Carex* sect. *Capituligerae*, Cyperaceae). *Journal of Biogeography*, *42*, 1514–1525.

Vonlanthen, P., Bittner, D., Hudson, A. G., Young, K. A., Müller, R., Lundsgaard-Hansen, B., … Seehausen, O. (2012). Eutrophication causes speciation reversal in whitefish adaptive radiations. *Nature*, *482*, 357–362.

Walther, G.-R. (2003). Plants in a warmer world. *Perspectives in Plant Ecology, Evolution and Systematics*, *6*, 169–185.

Walther, G.-R., Beißner, S., & Burga, C. A. (2005). Trends in the upward shift of alpine plants. *Journal of Vegetation Science*, *16*, 541–548.

Webb, W. C., Marzluff, J. M., & Omland, K. E. (2011). Random interbreeding between cryptic lineages of the Common Raven: Evidence for speciation in reverse. *Molecular Ecology*, *20*, 2390–2402.

Whitkus, R. (1988). Experimental hybridizations among chromosome races of *Carex pachystachya* and the related species *C. macloviana* and *C. preslii* (Cyperaceae). *Systematic Botany*, *13*, 146–153.

Whitkus, R. (1992). Allozyme variation within the *Carex pachystachya* complex (Cyperaceae). *Systematic Botany*, *17*, 16–24.

Whitney, K. D., Randell, R. A., & Rieseberg, L. H. (2010). Adaptive introgression of abiotic tolerance traits in the sunflower *Helianthus annuus*. *The New Phytologist*, *187*, 230–239.

Zink, R. M., Klicka, J., & Barber, B. R. (2004). The tempo of avian diversification during the Quaternary. *Philosophical Transactions of the Royal Society of London. Series B*, *359*, 215–220.

SUPPORTING INFORMATION

Additional Supporting Information may be found online in the supporting information tab for this article.

How to cite this article: Maguilla E, Escudero M, Hipp AL, Luceño M. Allopatric speciation despite historical gene flow: Divergence and hybridization in *Carex furva* and *C. lucennoiberica* (Cyperaceae) inferred from plastid and nuclear RAD-seq data. *Mol Ecol*. 2017;26:5646–5662. https://doi.org/10.1111/mec.14253